Published in final edited form as:
Immunity. 2012 January 27; 36(1): 68–78. doi:10.1016/j.immuni.2011.12.007.

Mitochondrial Respiratory Capacity Is A Critical Regulator Of CD8+ T Cell Memory Development

Gerritje J.W. van der Windt[1,2], **Bart Everts**[1,2], **Chih-Hao Chang**[1,2], **Jonathan D. Curtis**[1,2], **Tori C. Freitas**[1], **Eyal Amiel**[1], **Edward J. Pearce**[1,2], and **Erika L. Pearce**[1,2]

[1]Trudeau Institute, Saranac Lake, NY 12983, USA

Summary

$CD8^+$ T cells undergo major metabolic changes upon activation, but how metabolism influences the establishment of long-lived memory T (T_M) cells after infection remains a key question. We have shown here that $CD8^+$ T_M cells, but not effector $CD8^+$ (T_E) cells, possessed substantial mitochondrial spare respiratory capacity (SRC). SRC is the extra capacity available in cells to produce energy in response to increased stress or work and as such is associated with cellular survival. We found that interleukin-15 (IL-15), a cytokine critical for $CD8^+$ T_M cells, regulated SRC and oxidative metabolism by promoting mitochondrial biogenesis and expression of carnitine palmitoyl transferase (CPT1a), a metabolic enzyme that controls the rate-limiting step to mitochondrial fatty acid oxidation (FAO). These results show how cytokines control the bioenergetic stability of T_M cells after infection by regulating mitochondrial metabolism.

Introduction

$CD8^+$ T cells play a crucial role in immunity to infection and cancer. In response to antigen (Ag) and co-stimulation, $CD8^+$ T cells undergo a developmental program characterized by distinct phases encompassing first the expansion, and then contraction, of Ag-specific effector T (T_E) cell populations, followed by the persistence of long-lived memory T (T_M) cells that mediate immunity to re-infection (Harty and Badovinac, 2008). While this predictable pattern of the response is well characterized, the mechanisms underlying the generation and maintenance of $CD8^+$ T_M cells, and in particular how metabolism influences this process, remain unclear.

Upon activation T cells undergo a metabolic switch to glycolysis, which is required to support their growth, proliferation, and effector functions (Krauss et al., 2001; Rathmell et al., 2000; Roos and Loos, 1973). Conventional views suggest that proliferating T cells ferment glucose to make ATP, even though there is sufficient oxygen present to support oxidative phosphorylation (OXPHOS) (Brand and Hermfisse, 1997; Greiner et al., 1994; Wang et al., 1976), a phenomenon known as the Warburg effect (Warburg, 1956). Signals from IL-2 and co-stimulatory CD28 support the activation and expansion of T cells by

Address correspondence to EL Pearce, Department of Pathology & Immunology, Washington University School of Medicine, St. Louis, MO, 63110. Tel: 314 286 2509; Fax: 314 362 9108; erikapearce@path.wustl.edu.
[2]Current Address: Department of Pathology & Immunology, Washington University School of Medicine, St. Louis, MO, 63110, USA.

promoting this metabolic phenotype (Frauwirth et al., 2002; Wieman et al., 2007). In contrast to the glycolytic metabolism of T cells proliferating in response to Ag, it is thought that quiescent T cells (e.g. naive and T_M cells), like most cells in normal tissues, use OXPHOS to meet energy demands (Krauss et al., 2001) by interchangeably breaking down glucose, amino acids, and fats to fuel the tricarboxylic acid (TCA) cycle and ATP production (Fox et al., 2005; Jones and Thompson, 2007). Implicit in this divergence in metabolism between activated and quiescent T cells is that the conversion, or switching, between differing metabolic states is required to effectively generate a given T cell fate. This has clearly been shown to be the case for the switch to glycolysis that accompanies naïve T cell activation (Fox et al., 2005; Jones and Thompson, 2007). While it is known that growth factor cytokines support the survival of resting T cells, how cells attain a quiescent state, and the accompanying metabolic transformation to OXPHOS that would presumably occur during the development of stable $CD8^+$ T_M cells after infection is incompletely understood.

Previously we demonstrated that pharmacological modulation of fatty acid oxidation (FAO) enhanced $CD8^+$ T_M development after vaccination (Pearce et al., 2009). However, understanding the metabolic features of $CD8^+$ T_M cells, and the mechanistic insight into why FAO is critical for $CD8^+$ T_M, is still lacking. Using extracellular flux analysis we investigated the metabolism of T cells after infection in real time and discovered a striking mitochondrial marker that is unique to $CD8^+$ T_M cells. We show here that $CD8^+$ T_M cells, unlike $CD8^+$ T_E cells or resting naïve $CD8^+$ T cells, maintained substantial spare respiratory capacity (SRC) in their mitochondria. SRC is the extra mitochondrial capacity available in a cell to produce energy under conditions of increased work or stress and is thought to be important for long-term cellular survival and function (Choi et al., 2009; Ferrick et al., 2008; Nicholls, 2009; Nicholls et al., 2010; Yadava and Nicholls, 2007). We show here that SRC in $CD8^+$ T_M cells was dependent upon the ability of the cells to oxidize fats in their mitochondria. We demonstrate that IL-15, a cytokine critical for $CD8^+$ T_M cells (Kennedy et al., 2000; Ku et al., 2000; Mitchell et al., 2010; Sandau et al., 2010; Schluns et al., 2002; Surh and Sprent, 2008; Tan et al., 2002; Zhang et al., 1998), enhanced SRC by promoting mitochondrial biogenesis and the expression of carnitine palmitoyl transferase 1a (CPT1a), a mitochondrial protein which has been shown to play an important role in the utilization of fatty acids as an alternative energy source (Deberardinis et al., 2006; Ramsay and Zammit, 2004; Zaugg et al., 2011). Our genetic experiments show that CPT1a, and thus FAO, regulated SRC and $CD8^+$ T_M development. Our data indicate that maintaining mitochondrial function and SRC in $CD8^+$ T cells is key to stable $CD8^+$ T_M formation after infection.

Results

$CD8^+$ T_M cells have substantial mitochondrial spare respiratory capacity

To establish how cellular metabolism is regulated during an immune response we measured the bioenergetic profiles of naïve (T_N) $CD8^+$ T cells, and T_E and T_M $CD8^+$ T cells from wild-type (WT) mice infected with *Listeria monocytogenes*, in a basal state and after the addition of oligomycin (to block ATP synthesis), FCCP (to uncouple ATP synthesis from the electron transport chain, ETC), and rotenone and antimycin A (to block complex I and III of the ETC, respectively) (Figure S1A) (Gerencser et al., 2009; Nicholls et al., 2010). We found that the O_2 consumption rate (OCR), an indicator of OXPHOS (Figure S1B), was slightly higher in T_M cells in the basal state when compared to T_E and T_N cells (Figure 1A), while the basal extracellular acidification rate (ECAR), a consequence of lactic acid production (which is a marker of glycolysis), was greatest in T_E cells (Figure 1B). Strikingly however, T_M cells demonstrated a substantially larger mitochondrial SRC when compared to T_E and T_N cells, as indicated by the difference between the maximal OCR (after FCCP injection) and basal OCR (Figure 1A; Figure S1B).

$CD8^+$ T_M cells are characterized by their ability to persist for long periods of time and to respond vigorously to antigen re-encounter (Prlic et al., 2007). Since SRC is thought to be important for cellular survival and function (Choi et al., 2009; Ferrick et al., 2008; Nicholls, 2009; Nicholls et al., 2010; Yadava and Nicholls, 2007) we explored the role of SRC in $CD8^+$ T cells. We investigated whether the cytokines IL-2 and IL-15, which are critical for the development and maintenance of $CD8^+$ T_E and T_M cells, respectively (Kennedy et al., 2000; Mitchell et al., 2010; Sandau et al., 2010; Schluns et al., 2002; Surh and Sprent, 2008; Tan et al., 2002; Zhang et al., 1998), influence SRC. We isolated $CD8^+$ T cells from major histocompatibility (MHC) class I-restricted OT-I transgenic mice and measured their bioenergetic profiles after stimulation with OVA peptide and IL-2 for 3 days, followed by 4 days of culture in either IL-2 or IL-15 (Figure 1C) (Carrio et al., 2004). These *in vitro* culture conditions approximate the program of T_E and T_M development after the response to an infection *in vivo*. Upon infection, antigen and IL-2 promote $CD8^+$ T_E activation and proliferation, followed by the contraction of these cell populations as infection is cleared and antigen and growth factors such as IL-2 decline. During this time presumably, exposure to cytokines such as IL-15 promotes the development and maintenance of $CD8^+$ T_M cells (Sandau et al., 2010; Schluns et al., 2002; Zhang et al., 1998). Culture with IL-2 and IL-15 induced T_E-like (IL-2 T_E) and T_M-like (IL-15 T_M) cells respectively, which displayed activation marker phenotypes similar to T_E and T_M cells generated after infection (Figure S1C) (Carrio et al., 2004). Consistent with the idea that proliferating T cells use glycolysis for energy (Frauwirth et al., 2002; Jones and Thompson, 2007) we found that IL-2 T_E cells displayed high basal ECAR (Figure 1D) when compared to IL-15 T_M cells. In contrast, while IL-15 T_M cells were less metabolically active in a basal state, as shown by lower basal ECAR (Figure 1D) and OCR (Figure S1D) when compared to IL-2 T_E cells, they possessed a higher OCR/ECAR ratio (Figure 1E). This would indicate that IL-15 T_M cells preferentially use OXPHOS rather than glycolysis. We found that IL-15 promoted SRC in activated $CD8^+$ T cells, whereas $CD8^+$ T cells cultured in the presence of IL-2 lacked this energy reserve (Figure 1F). In addition, to rule out effects from substrate limitations during the assay, we performed the assay in the absence or presence of 10% serum and observed similar results (data not shown). Consistent with the idea that SRC is an intrinsic feature of $CD8^+$ T_M cells, we found that culture with IL-7, which also promotes the development of $CD8^+$ T_M-like cells *in vitro* (Carrio et al., 2004), and is important for the $CD8^+$ T_M cell homeostasis *in vivo* (Tan et al., 2002), enhanced SRC (data not shown).

To determine how SRC correlates with the ability to produce energy in response to increased work, we re-stimulated IL-2 T_E and IL-15 T_M cells with anti-CD3 and anti-CD28, and found that IL-15 T_M cells have an increased amount of ATP after re-stimulation when compared to IL-2 T_E cells (Figure 2A). Moreover, upon re-stimulation IL-2 T_E cells had decreased mitochondrial membrane potential (Ψ_{mito}) and enhanced superoxide production (Figures S2A and S2B), two parameters that indicate poor mitochondrial health (Grayson et al., 2003; Lambert and Brand, 2009; Mookerjee et al., 2010). Meanwhile IL-15 T_M cells showed increased Ψ_{mito} and lower superoxide concentration. Consistent with this, IL-15 T_M cells survived better (Figure S2C) after re-stimulation when compared to IL-2 T_E cells. Since upon re-stimulation T_M cells should convert to a T_E phenotype, we tested whether re-stimulating IL-15 T_M cells resulted in a metabolic switch from OXPHOS to glycolysis. Indeed, upon stimulation with PMA and ionomycin, IL-15 T_M cells rapidly increased their ECAR (Figure S2D), and decreased their OCR/ECAR ratio (Figure S2E), while a longer stimulation with anti-CD3 and anti-CD28 also resulted in a lower OCR/ECAR ratio (Figure S2F) in those cells. Since all cells in these cultures were first activated with OVA peptide in the presence of IL-2, we wanted to establish that signals from IL-15, rather than simply the withdrawal of IL-2, regulated $CD8^+$ T cell survival. Indeed we found that Bcl-2 expression, which correlates with $CD8^+$ T cell survival (Grayson et al., 2000), was highest in IL-15 T_M cells (Figure 2B), and that $CD8^+$ T cells after IL-2 withdrawal were not long-lived without

signals from IL-15 (Figure 2C). To explore whether IL-15 T_M cells survived better *in vivo*, we adoptively transferred IL-2 T_E cells or IL-15 T_M cells into congenic mice and after 2 days we found significantly more IL-15 T_M than IL-2 T_E donor cells in spleen and lymph nodes (Figure 2D), which is consistent with data showing that IL-15 is critical for $CD8^+$ T cell persistence (Kennedy et al., 2000; Sandau et al., 2010; Schluns et al., 2002). Together the data suggest that enhanced SRC enables T_M cells to survive as functional long-lived cells and that this process is modulated by IL-15.

IL-15 induces mitochondrial biogenesis in $CD8^+$ T cells

Since SRC is a measure of how efficiently the ETC can move protons from the mitochondrial matrix into the intermembrane space in the presence of the uncoupler FCCP as compared to the basal state (Figure S1A) (Mookerjee et al., 2010; Nicholls et al., 2010), we reasoned that the enhanced SRC evident in IL-15 T_M cells might be explained by an increase in mitochondrial mass. IL-2 T_E cells are larger than IL-15 T_M cells (Carrio et al., 2004; Rathmell et al., 2000), and we found that their larger cytoplasm had a dispersed mitochondrial distribution (Figure 3A). In contrast, IL-15 T_M cells had a smaller cytoplasmic space with tightly packed mitochondria, indicating a difference in the ratio between mitochondrial mass and total cell mass between T_E and T_M cells (Figure 3A and Figure S3). We next tested whether IL-15 induced mitochondrial biogenesis in $CD8^+$ T cells by quantifying the ratio of mitochondrial DNA to nuclear DNA (mtDNA/nDNA) and found that this ratio was higher in IL-15 T_M cells than in IL-2 T_E cells (Figure 3B). We also found that IL-15 T_M cells expressed more ETC protein complex I (Figure 3C), which has previously been reported to be important for T_M cell function (Yi et al., 2006), Moreover, IL-15 T_M cells had greater expression of mitochondrial transcription factor A (TFAM) mRNA (Figure 3D). Together these data demonstrate the enhanced mitochondrial content of IL-15 T_M cells. NADH is generated by the TCA cycle and donates electrons to complex I as part of OXPHOS (Saraste, 1999) (Figure S1A). To test whether enhanced NADH availability further contributes to the greater SRC in IL-15 T_M cells we measured the amount of NAD(H) (total NAD^+ and NADH) and found that IL-15 T_M cells actually had less NADH, as demonstrated by a lower amount of total NAD(H) and a higher NAD/NADH ratio, than IL-2 T_E cells (Figure 3E). Importantly, when NADH consumption by the ETC was blocked with rotenone and antimycin A, IL-15 T_M cells accumulated more NADH than IL-2 T_E cells (Figure 3F). This would suggest that IL-15 T_M cells preferentially use OXPHOS to generate energy, correlating with our results showing that IL-15 T_M cells have higher OCR/ECAR ratios (Figure 1E). Together these data show that IL-15 induces mitochondrial biogenesis in $CD8^+$ T cells and that greater mitochondrial mass, rather than greater NADH availability, contributes to enhanced SRC in these IL-15 T_M cells.

To confirm that *bona fide* $CD8^+$ T_M cells isolated after *L. monocytogenes* infection had enhanced mitochondrial content, we quantified the ratio of mtDNA/nDNA and found that this ratio was higher in $CD8^+$ T_M cells than in $CD8^+$ T_E cells (Figure 4A). Notably, $CD8^+$ T_N cells had fewer mitochondria than T_M cells, indicating that enhanced mitochondrial mass is not a characteristic of resting T cells in general, but is unique to T_M cells. This correlates with our finding that only T_M cells, and not T_N and T_E cells, have considerable SRC. In addition, *bona fide* $CD8^+$ T_M cells had a denser mitochondrial distribution, while mitochondria in $CD8^+$ T_E cells were generally more disperse (Figure 4B). We also found that $CD8^+$ T_M cells had significantly higher TFAM mRNA (Figure 4C) and complex I protein expression when compared to $CD8^+$ T_E cells (Figure 4D). Together our data indicate that $CD8^+$ T_M cells have greater mitochondrial mass and this underlies their enhanced SRC.

Spare respiratory capacity in CD8$^+$ T cells is dependent on mitochondrial fatty acid oxidation

Our previous studies showed that pharmacologically modulating FAO after infection could promote the generation of CD8$^+$ T_M cells (Pearce et al., 2009). Since IL-15 is known to promote T_M development (Sandau et al., 2010; Schluns et al., 2002; Zhang et al., 1998), and we have shown here that IL-15 supports SRC in CD8$^+$ T cells, we sought to determine whether IL-15-enhanced SRC is associated with mitochondrial FAO. The rate-limiting step to FAO is the transfer of fatty acids from the cytosol into mitochondria by carnitine palmitoyltransferase 1 (CPT1) (Deberardinis et al., 2006; Ramsay and Zammit, 2004). We measured CPT1a mRNA in IL-2 T_E and IL-15 T_M cells and found that IL-15 T_M cells expressed more CPT1a mRNA (Figure 5A). This indicates that IL-15 promotes the use of fatty acids for energy, and correlates with our finding that IL-15 induces mitochondrial biogenesis.

To determine whether the enhanced SRC in IL-15 T_M cells depends on FAO we exposed IL-15 T_M cells to the CPT1 inhibitor etomoxir, which blocks mitochondrial FAO (Deberardinis et al., 2006; Lopaschuk et al., 1988). Treatment with etomoxir, either before or after FCCP injection, impaired SRC in IL-15 T_M cells (Figure 5B). Also evident is that basal OCR was inhibited by etomoxir (Figure 5B, left panel), further demonstrating that IL-15 T_M cells use FAO for energy in a resting state. In contrast, OCR in IL-2 T_E cells was not affected by etomoxir (Figure 5C). Consistent with these findings, SRC in *bona fide* CD8$^+$ T_M cells isolated after *L. monocytogenes* infection was also impaired by etomoxir, whereas the OCR after FCCP in CD8$^+$ T_E cells was not affected (Figure 5D). To test whether the inhibition of FAO alters the survival of IL-15 T_M cells *in vitro*, we cultured cells with etomoxir and found that CPT1a inhibition impaired their survival (Figure S4).

To further substantiate that SRC is regulated by FAO we next used a genetic approach. We modulated the expression of CPT1a by transducing CD8$^+$ T cells with retrovirus expressing shRNA against CPT1a (hpCPT1a), and found that inhibiting CPT1a expression in IL-15 T_M cells reduced maximum OCR after injection of FCCP (Figure 6A), while hpCPT1a expression did not affect maximum OCR in IL-2 T_E cells (Figure 6B). To assess the effect of a genetic gain of function for FAO, we retrovirally expressed CPT1a (CPT1a EX) in CD8$^+$ T cells. Retroviral expression of CPT1a significantly enhanced maximal OCR after FCCP in both IL-15 T_M cells (Figure 6C) and IL-2 T_E cells (Figure 6D). The same results were found when the data were expressed as SRC (Figure 6A-D, where maximum OCR after FCCP is calculated as a percentage of baseline OCR). The efficacy of the hpCPT1a and CPT1a EX to modulate the expression of CPT1a was confirmed (Figure S5A). We further verified that CPT1a EX directly promoted FAO by showing that etomoxir inhibits the enhanced maximum OCR in CPT1a EX IL-15 T_M cells to a greater extent than in control IL-15 T_M cells (Figure S5B). Consistent with increased SRC, retroviral CPT1a expression enhanced the survival of IL-15 T_M cells *in vitro* (Figure S5C). Together these data establish that increased FAO positively regulates SRC in CD8$^+$ T cells and thereby favors cellular survival.

Mitochondrial FAO enhances T cell survival and promotes CD8$^+$ T_M cell development

To explore whether CPT1a, and thus FAO, supports Ag-specific CD8$^+$ T cell survival *in vivo*, we adoptively transferred activated control-transduced or CPT1a EX-transduced OT-I T cells into congenic mice and found significantly more CPT1a EX-transduced donor cells in spleen and lymph nodes than control-transduced donor cells after 2 days (Figure 7A), indicating that CPT1a increases survival of Ag-specific CD8$^+$ T cells *in vivo*. Finally, to establish that FAO regulates development of CD8$^+$ T_M cells we adoptively transferred activated control-transduced and CPT1a-EX-transduced OT-I T cells into congenic

recipients and tracked OVA-specific $CD8^+$ T cell responses after immunization with *L. monocytogenes*. The frequency of OVA-specific cells that are control-transduced remains the same from the T_E phase to the T_M phase (Figure 7B, compare 66% in T_E to 68% in T_M, contour plots and left bar graph), indicating that there was no advantage to expressing the control vector in promoting cell survival. However, the frequency of CPT1a EX-transduced cells significantly increased from the peak of the T_E response through contraction (Figure 7B, compare 58% in T_E to 87% in T_M, contour plots and left bar graph). The advantage to expressing the CPT1a EX vector was demonstrated by less contraction (Figure 7B, middle bar graph), and resulted in higher absolute numbers of CPT1a EX-transduced T_M cells as compared to control-transduced T_M cells, both in blood (Figure 7B, middle bar graph) and in spleen (Figure 7B, right bar graph). Furthermore, total T_M cells increased in mice that received adoptive transfers of CPT1a EX transduced cells, suggesting that the CPT1a pathway is a limiting factor in T_M cell generation (Figure S6A and S6B). Together, these data show that CPT1a, and thus FAO, promotes the development of $CD8^+$ T_M cells after infection.

To determine the extent to which the effects of IL-15 signals on $CD8^+$ T_M cells *in vivo* are CPT1a- dependent we adoptively transferred activated control-transduced and CPT1a-EX-transduced OT-I T cells into IL-15 deficient recipients and tracked OVA-specific $CD8^+$ T cell responses after immunization with *L. monocytogenes*. While the frequencies of control and CPT1a EX transduced cells were similar at the peak of the response (T_E), more CPT1a EX transduced cells survived contraction and subsequently were able to respond to a challenge infection (Figure 7C). We found, however, that the survival of both control and CPT1a EX transduced cells was reduced in IL-15 deficient recipients when compared to WT recipient mice (Figure S6C). These results suggest that IL-15 signals promote CPT1a expression and FAO to support $CD8^+$ T_M cells, but that this is not the only function of IL-15.

Discussion

We propose a model where mitochondrial respiratory capacity regulates T cell survival after infection. As T_E cells undergo clonal expansion during an immune response they primarily use glycolysis to support rapid cell growth. We speculate that during this process the majority of $CD8^+$ T_E cells fail to maintain and/or induce mitochondrial biogenesis and this results in a reduction in the ratio between mitochondrial mass and overall cell mass, and a consequential loss of reserve energy-generating capacity, i.e. SRC. Reduced mitochondrial mass increases dependence on glycolysis and renders T_E cells bioenergetically unstable as they lose the ability to create energy from diverse substrates via OXPHOS, and thus are unable to maintain viability when infection associated signals decline and elements such as IL-2 that support glycolysis dissipate. Some Ag-specific T cells from the primary infection survive as long-lived T_M cells because they maintain mitochondrial mass via exposure to IL-15, or perhaps other common γ cytokines such as IL-7. Since FAO occurs in mitochondria, more mitochondrial mass allows greater use of fatty acids for energy via OXPHOS, thereby facilitating cell survival in the absence of pro-glycolysis signals. Moreover, the enhanced SRC provided by increased mitochondrial mass, might allow T_M cells to respond quickly (“rapid recall”) if pathogen is reencountered.

Whether T cells receive growth factor signals can be controlled at many levels, including cytokine and cytokine receptor expression, trans-presentation of the cytokine to the T cells by antigen presenting cells or other accessory cells (McGill et al., 2010; Stonier et al., 2008), or T cell localization to niches where a cytokine is expressed. It is likely that whether T cells are able to receive signals from growth factors *in vivo* is a result of a combination of these mechanisms. Our preliminary observations indicate that lymph node homing receptors are

upregulated immediately upon IL-2 withdrawal *in vitro*, suggesting that once infection associated signals such as IL-2 dissipate, cells become competent to traffic to lymph nodes where they gain access to IL-15 or IL-7. Additionally, it has been shown that Ag-specific $CD8^+$ cells that have not fully differentiated into terminal T_E cells during primary infection express IL-7R and persist as long-lived T_M cells (Kaech et al., 2003). This suggests the possibility that these T cells have maintained mitochondrial function throughout contraction because of continual signals from IL-7.

The IL-2 and IL-15 receptors share identical subunits and their signaling pathways overlap (Hofmann et al., 2002; Waldmann et al., 1998), implying that the strength of signal through the cytokine receptor, rather than the mere induction of these pathways, may lead to the differential effects of IL-2 compared to IL-15 on T_E cells versus T_M cell differentiation (Carrio et al., 2004). However, our unpublished observations suggest that overall Stat5 phosphorylation is similar between our cultured IL-2 T_E and IL-15 T_M cells, indicating that at least the degree of Stat5 activation *per se* is not sufficient to dictate the differential effects of these cytokines. More work needs to be done to determine whether there is a unique signaling element, perhaps shared by IL-15 and IL-7 that supports T_M cell development (Carrio et al., 2004).

Our data showing that retroviral expression of CPT1a facilitates $CD8^+$ T_M development in IL-15 deficient mice, but not to the same extent as in WT recipients, suggest that while IL-15 does promote FAO to support T_M cells that this is not the only function of IL-15 during an immune response. We speculate that mitochondrial biogenesis is key to stable T_M cell formation and that this is regulated by IL-15. While CPT1a EX transduced cells increase FAO due to enhanced CPT1a expression, they lack the mitochondrial mass, and thus energy producing machinery to maintain full bioenergetic stability when in an IL-15 deficient environment.

While we believe that our findings show how metabolism regulates T cell responses after infection, several questions remain. For example, how do T_E cells come to have less SRC than T_M cells? Although it has been described that mitochondrial biogenesis is up-regulated early after $CD8^+$ T cell activation (D'Souza et al., 2007), we speculate that Ag-specific T_E cells that continue to proliferate during infection might eventually outpace their own mitochondrial biogenesis, explaining why T_E cells have less mitochondrial mass. It is also possible that mitochondria segregate unequally as T cells asymmetrically divide so that terminally differentiated T_E cells acquire fewer mitochondria (Chang et al., 2007). Another unresolved issue is that of why T_N cells have less SRC than T_M cells. We have shown here that T_N have less mitochondrial mass than T_M cells, which correlates with their decreased SRC. It is also possible that qualitative differences exist between the mitochondria in T_N and T_M cells, such as differences in expression of ETC complexes on a per mitochondrion basis, which could in part be explained by the effects of IL-15 on T_M cells after infection. This suggests that cell-intrinsic bioenergetic differences underlie the disparity in functionality between T_N and T_M cells, i.e. the rapid recall of T_M cells is possible because of enhanced SRC. All of these areas are actively under study.

Agents that protect cells against loss in mitochondrial SRC, or that induce mitochondrial biogenesis, are thought to have potential for treating numerous pathologies (Beeson et al., 2010). Our findings here suggest that drugs that target mitochondrial SRC could hold promise as immunotherapeutics and might warrant further study for their ability to alter T cell responses. These results may serve to focus scientific efforts toward investigating how mitochondria dictate T cell function and lifespan, and thus impact how successful therapies and vaccines are designed.

Experimental Procedures

Mice and immunizations

C57BL/6, C57BL/6 CD45.1, C57BL/6 CD90.1, and major histocompatibility-complex class-I-restricted OVA specific T-cell-receptor (OT-I) transgenic mice were purchased from The Jackson Laboratory, and re-derived stocks were maintained at the Trudeau Institute under specific pathogen-free conditions under protocols approved by the Institutional Animal Care and Use Committee. IL-15 deficient mice (IL-$15^{-/-}$) were purchased from Taconic. We used the attenuated strain of recombinant *Listeria monocytogenes* deleted for actA (LmOVA) for immunizations. Mice were infected intravenously or intraperitoneally with a sub-lethal dose of 1×10^7 to 5×10^7 colony forming units (CFU), and if indicated challenge infected with 5×10^7 CFU (Pearce et al., 2009). T_N, T_E and T_M cell isolations from spleens and lymph nodes were done based on $CD8^+$, CD44 and CD62L expression ($CD44^{lo}$ $CD62L^{hi}$, $CD44^{hi}$ $CD62L^{lo}$ and $CD44^{hi}$ $CD62L^{hi}$, respectively) or donor marker, at 6–7 days (T_E) or 14–40 days (T_M) after infection, using the BD Influx sorter or MACS purification (Miltenyi Biotech).

Flow cytometry

All fluorochrome-conjugated monoclonal antibodies were purchased from BD Pharmingen or eBioscience. All staining was performed as previously described (Pearce et al., 2009). OVA-specific $CD8^+$ T cells were quantified by direct staining with H2-K^b $OVA_{257–264}$ (K^bOVA) MHC–peptide tetramers, either by killing animals and collecting cells from organs or by collecting blood from live animals (serial bleeds), as indicated. Mitochondrial membrane potential was measured using 3,3'-dihexyloxacarbocyanine iodide ($DiOC_6$) (Invitrogen) and superoxide production using dihydroethidium (HE) (Sigma).

In vitro cultures and retroviral transductions

OT-I splenocytes were activated with OVA-peptide and IL-2 (100 U/ml) for 3 days, and subsequently cultured in the presence of either IL-2 or IL-15 (10 ng/ml) for 4 days. For restimulation assays, activated T cells were re-activated with either anti-CD3 (5.0 μg/ml) + anti-CD28 (0.5 μg /ml). For retroviral transduction experiments, OT-I splenocytes were activated, transduced with control (empty vector or virus expressing shRNA against luciferase), CPT1a expressing virus (CPT1a EX), or virus expressing shRNA against CPT1a (hpCPT1a) 1 day later, and subsequently cultured as described. GFP is a marker of retroviral expression. For *in vitro* survival assays, OT-I splenocytes were activated for 3 days as described, then plated (1×10^5 cells) in a 96-well plate in the presence of the indicated cytokine and (if indicated) 200 μM etomoxir, and daily analyzed for 7-AAD staining.

Adoptive transfers

For adoptive transfer experiments, naïve OT-I cells were obtained from the blood or spleen, K^bOVA tetramers were used to determine numbers of OT-I cells, and then $1–3\times10^4$ OT-I cells, were transferred into CD45.1 or CD90.1 congenic recipient mice. For in vivo survival analysis of cultured IL-2 T_E and IL-15 T_M cells, 1×10^6 cells were transferred into congenic recipient mice. For adoptive transfer of retrovirally transduced OT-I cells for *in vivo* survival analysis, GFP^+ cells were sorted and 1×10^6 cells were transferred into CD45.1 congenic recipient mice. For adoptive transfer of retrovirally transduced OT-I cells for T_M development, 1×10^5 GFP^+ cells were transferred into CD45.1 congenic or IL-15 deficient recipient mice.

Metabolism assays

Oxygen consumption rates (OCR) and extracellular acidification rates (ECAR) were measured in XF media (non-buffered RPMI 1640 containing 25 mM glucose, 2 mM L-glutamine and 1 mM sodium pyruvate), under basal conditions and in response to 200 μM etomoxir, 1 μM oligomycin, 1.5 μM fluoro-carbonyl cyanide phenylhydrazone (FCCP) and 100 nM rotenone + 1 μM antimycin A (Sigma), or PMA (50 ng/ml) + ionomycin (500 ng/ml) using the XF-24 Extracellular Flux Analyzer (Seahorse Bioscience). NAD(H) measurements were performed using the NAD^+ and NADH Quantification Kit (BioVision), and ATP measurements using the ATP determination kit (Invitrogen).

Imaging

IL-2 T_E and IL-15 T_M cells were stained for CD8 (BD bioscience), Mitotracker green and Hoechst (Invitrogen). T_N, T_E and T_M cells were sorted by CD44, CD8, and CD62L after *L. monocytogenes* infection, and stained with Mitotracker green and Hoechst.

RT-PCR and western blot analysis

RNA isolations were done using the RNeasy kit (Qiagen) and single strand cDNA was synthesized using High Capacity cDNA Reverse Transcription Kit (Applied Biosystems). Genomic DNA was extracted using the phenol-chloroform method to determine mtDNA/nDNA ratios (Guo et al., 2009). Primers were purchased from Applied Biosystems and real-time PCR was performed by the Taqman method using an Applied Biosystems 7500 sequence detection system. The expression of mRNA for genes of interest was normalized to the expression of a housekeeping gene (GAPDH). Cell lysate preparation, SDS–PAGE, electrophoretic transfer, immunoblotting and development using enhanced chemiluminescence were accomplished as previously described (Pearce et al., 2009). The Complex I antibody (subunit NDUFB8) for western analysis was purchased from Mitosciences.

Statistical analysis

Comparisons for two groups were calculated using unpaired two-tailed Student's *t*-tests, comparisons for more than two groups were calculated using 1-way ANOVA followed by Bonferroni's multiple comparison tests. Comparisons over time were calculated using 2-way ANOVA followed by Bonferroni's multiple comparison tests.

Supplementary Material

Refer to Web version on PubMed Central for supplementary material.

Acknowledgments

We thank Mike Tighe, Debbie Duso, Ron Lacourse, Brandon Sells, and Georgia Perona-Wright for technical assistance, and David Woodland and Jake Kohlmeier for critical reading of the manuscript. This work was supported in part by the Trudeau Institute, and grants from the NIH (E.L.P, E.J.P), NIAID Institutional Training Grant (E.A.), Netherlands Organisation for Scientific Research (G.J.W.W.) and the Emerald Foundation (E.L.P). There are no conflicts of interest. G.J.W.W., B.E., J.D.C., E.A., E.J.P., and E.L.P. designed the research and analyzed the data. G.J.W.W., B.E., C.H.C, J.D.C., T.C.F. and E.L.P. performed experiments. G.J.W.W., B.E., E.J.P., and E.L.P. contributed to the preparation of the manuscript. G.J.W.W. wrote the manuscript with E.L.P.

References

Beeson CC, Beeson GC, Schnellmann RG. A high-throughput respirometric assay for mitochondrial biogenesis and toxicity. Anal Biochem. 2010; 404:75–81. [PubMed: 20465991]

Brand KA, Hermfisse U. Aerobic glycolysis by proliferating cells: a protective strategy against reactive oxygen species. FASEB J. 1997; 11:388–395. [PubMed: 9141507]

Carrio R, Bathe OF, Malek TR. Initial antigen encounter programs CD8+ T cells competent to develop into memory cells that are activated in an antigen-free, IL-7- and IL-15-rich environment. J Immunol. 2004; 172:7315–7323. [PubMed: 15187107]

Chang JT, Palanivel VR, Kinjyo I, Schambach F, Intlekofer AM, Banerjee A, Longworth SA, Vinup KE, Mrass P, Oliaro J, et al. Asymmetric T lymphocyte division in the initiation of adaptive immune responses. Science. 2007; 315:1687–1691. [PubMed: 17332376]

Choi SW, Gerencser AA, Nicholls DG. Bioenergetic analysis of isolated cerebrocortical nerve terminals on a microgram scale: spare respiratory capacity and stochastic mitochondrial failure. J Neurochem. 2009; 109:1179–1191. [PubMed: 19519782]

D'Souza AD, Parikh N, Kaech SM, Shadel GS. Convergence of multiple signaling pathways is required to coordinately up-regulate mtDNA and mitochondrial biogenesis during T cell activation. Mitochondrion. 2007; 7:374–385. [PubMed: 17890163]

Deberardinis RJ, Lum JJ, Thompson CB. Phosphatidylinositol 3-kinase-dependent modulation of carnitine palmitoyltransferase 1A expression regulates lipid metabolism during hematopoietic cell growth. J Biol Chem. 2006; 281:37372–37380. [PubMed: 17030509]

Ferrick DA, Neilson A, Beeson C. Advances in measuring cellular bioenergetics using extracellular flux. Drug Discov Today. 2008; 13:268–274. [PubMed: 18342804]

Fox CJ, Hammerman PS, Thompson CB. Fuel feeds function: energy metabolism and the T-cell response. Nat Rev Immunol. 2005; 5:844–852. [PubMed: 16239903]

Frauwirth KA, Riley JL, Harris MH, Parry RV, Rathmell JC, Plas DR, Elstrom RL, June CH, Thompson CB. The CD28 signaling pathway regulates glucose metabolism. Immunity. 2002; 16:769–777. [PubMed: 12121659]

Gerencser AA, Neilson A, Choi SW, Edman U, Yadava N, Oh RJ, Ferrick DA, Nicholls DG, Brand MD. Quantitative microplate-based respirometry with correction for oxygen diffusion. Anal Chem. 2009; 81:6868–6878. [PubMed: 19555051]

Grayson JM, Laniewski NG, Lanier JG, Ahmed R. Mitochondrial potential and reactive oxygen intermediates in antigen-specific CD8+ T cells during viral infection. J Immunol. 2003; 170:4745–4751. [PubMed: 12707355]

Grayson JM, Zajac AJ, Altman JD, Ahmed R. Cutting edge: increased expression of Bcl-2 in antigen-specific memory CD8+ T cells. J Immunol. 2000; 164:3950–3954. [PubMed: 10754284]

Greiner EF, Guppy M, Brand K. Glucose is essential for proliferation and the glycolytic enzyme induction that provokes a transition to glycolytic energy production. J Biol Chem. 1994; 269:31484–31490. [PubMed: 7989314]

Guo W, Jiang L, Bhasin S, Khan SM, Swerdlow RH. DNA extraction procedures meaningfully influence qPCR–based mtDNA copy number determination. Mitochondrion. 2009; 9:261–265. [PubMed: 19324101]

Harty JT, Badovinac VP. Shaping and reshaping CD8+ T-cell memory. Nat Rev Immunol. 2008; 8:107–119. [PubMed: 18219309]

Hofmann SR, Ettinger R, Zhou YJ, Gadina M, Lipsky P, Siegel R, Candotti F, O'Shea JJ. Cytokines and their role in lymphoid development, differentiation and homeostasis. Curr Opin Allergy Clin Immunol. 2002; 2:495–506. [PubMed: 14752332]

Jones RG, Thompson CB. Revving the engine: signal transduction fuels T cell activation. Immunity. 2007; 27:173–178. [PubMed: 17723208]

Kaech SM, Tan JT, Wherry EJ, Konieczny BT, Surh CD, Ahmed R. Selective expression of the interleukin 7 receptor identifies effector CD8 T cells that give rise to long-lived memory cells. Nat Immunol. 2003; 4:1191–1198. [PubMed: 14625547]

Kennedy MK, Glaccum M, Brown SN, Butz EA, Viney JL, Embers M, Matsuki N, Charrier K, Sedger L, Willis CR, et al. Reversible defects in natural killer and memory CD8 T cell lineages in interleukin 15-deficient mice. J Exp Med. 2000; 191:771–780. [PubMed: 10704459]

Krauss S, Brand MD, Buttgereit F. Signaling takes a breath--new quantitative perspectives on bioenergetics and signal transduction. Immunity. 2001; 15:497–502. [PubMed: 11672532]

Ku CC, Murakami M, Sakamoto A, Kappler J, Marrack P. Control of homeostasis of CD8+ memory T cells by opposing cytokines. Science. 2000; 288:675–678. [PubMed: 10784451]

Lambert AJ, Brand MD. Reactive oxygen species production by mitochondria. Methods Mol Biol. 2009; 554:165–181. [PubMed: 19513674]

Lopaschuk GD, Wall SR, Olley PM, Davies NJ. Etomoxir, a carnitine palmitoyltransferase I inhibitor, protects hearts from fatty acid-induced ischemic injury independent of changes in long chain acylcarnitine. Circ Res. 1988; 63:1036–1043. [PubMed: 3197271]

McGill J, Van Rooijen N, Legge KL. IL-15 trans-presentation by pulmonary dendritic cells promotes effector CD8 T cell survival during influenza virus infection. J Exp Med. 2010; 207:521–534. [PubMed: 20212069]

Mitchell DM, Ravkov EV, Williams MA. Distinct roles for IL-2 and IL-15 in the differentiation and survival of CD8+ effector and memory T cells. J Immunol. 2010; 184:6719–6730. [PubMed: 20483725]

Mookerjee SA, Divakaruni AS, Jastroch M, Brand MD. Mitochondrial uncoupling and lifespan. Mech Ageing Dev. 2010; 131:463–472. [PubMed: 20363244]

Nicholls DG. Spare respiratory capacity, oxidative stress and excitotoxicity. Biochem Soc Trans. 2009; 37:1385–1388. [PubMed: 19909281]

Nicholls DG, Darley-Usmar VM, Wu M, Jensen PB, Rogers GW, Ferrick DA. Bioenergetic profile experiment using C2C12 myoblast cells. J Vis Exp. 2010:46.

Pearce EL, Walsh MC, Cejas PJ, Harms GM, Shen H, Wang LS, Jones RG, Choi Y. Enhancing CD8 T-cell memory by modulating fatty acid metabolism. Nature. 2009; 460:103–107. [PubMed: 19494812]

Prlic M, Williams MA, Bevan MJ. Requirements for CD8 T-cell priming, memory generation and maintenance. Curr Opin Immunol. 2007; 19:315–319. [PubMed: 17433873]

Ramsay RR, Zammit VA. Carnitine acyltransferases and their influence on CoA pools in health and disease. Mol Aspects Med. 2004; 25:475–493. [PubMed: 15363637]

Rathmell JC, Vander Heiden MG, Harris MH, Frauwirth KA, Thompson CB. In the absence of extrinsic signals, nutrient utilization by lymphocytes is insufficient to maintain either cell size or viability. Mol Cell. 2000; 6:683–692. [PubMed: 11030347]

Roos D, Loos JA. Changes in the carbohydrate metabolism of mitogenically stimulated human peripheral lymphocytes. II. Relative importance of glycolysis and oxidative phosphorylation on phytohaemagglutinin stimulation. Exp Cell Res. 1973; 77:127–135. [PubMed: 4690164]

Sandau MM, Kohlmeier JE, Woodland DL, Jameson SC. IL-15 regulates both quantitative and qualitative features of the memory CD8 T cell pool. J Immunol. 2010; 184:35–44. [PubMed: 19949092]

Saraste M. Oxidative phosphorylation at the fin de siecle. Science. 1999; 283:1488–1493. [PubMed: 10066163]

Schluns KS, Williams K, Ma A, Zheng XX, Lefrancois L. Cutting edge: requirement for IL-15 in the generation of primary and memory antigen-specific CD8 T cells. J Immunol. 2002; 168:4827–4831. [PubMed: 11994430]

Stonier SW, Ma LJ, Castillo EF, Schluns KS. Dendritic cells drive memory CD8 T-cell homeostasis via IL-15 transpresentation. Blood. 2008; 112:4546–4554. [PubMed: 18812469]

Surh CD, Sprent J. Homeostasis of naive and memory T cells. Immunity. 2008; 29:848–862. [PubMed: 19100699]

Tan JT, Ernst B, Kieper WC, LeRoy E, Sprent J, Surh CD. Interleukin (IL)-15 and IL-7 jointly regulate homeostatic proliferation of memory phenotype CD8+ cells but are not required for memory phenotype CD4+ cells. J Exp Med. 2002; 195:1523–1532. [PubMed: 12070280]

Waldmann T, Tagaya Y, Bamford R. Interleukin-2, interleukin-15, and their receptors. Int Rev Immunol. 1998; 16:205–226. [PubMed: 9505189]

Wang T, Marquardt C, Foker J. Aerobic glycolysis during lymphocyte proliferation. Nature. 1976; 261:702–705. [PubMed: 934318]

Warburg O. On respiratory impairment in cancer cells. Science. 1956; 124:269–270. [PubMed: 13351639]

Wieman HL, Wofford JA, Rathmell JC. Cytokine stimulation promotes glucose uptake via phosphatidylinositol-3 kinase/Akt regulation of Glut1 activity and trafficking. Mol Biol Cell. 2007; 18:1437–1446. [PubMed: 17301289]

Yadava N, Nicholls DG. Spare respiratory capacity rather than oxidative stress regulates glutamate excitotoxicity after partial respiratory inhibition of mitochondrial complex I with rotenone. J Neurosci. 2007; 27:7310–7317. [PubMed: 17611283]

Yi JS, Holbrook BC, Michalek RD, Laniewski NG, Grayson JM. Electron transport complex I is required for CD8+ T cell function. J Immunol. 2006; 177:852–862. [PubMed: 16818739]

Zaugg K, Yao Y, Reilly PT, Kannan K, Kiarash R, Mason J, Huang P, Sawyer SK, Fuerth B, Faubert B, et al. Carnitine palmitoyltransferase 1C promotes cell survival and tumor growth under conditions of metabolic stress. Genes Dev. 2011; 25:1041–1051. [PubMed: 21576264]

Zhang X, Sun S, Hwang I, Tough DF, Sprent J. Potent and selective stimulation of memory-phenotype CD8+ T cells in vivo by IL-15. Immunity. 1998; 8:591–599. [PubMed: 9620680]

Highlights

- $CD8^+$ T_M cells possess substantial mitochondrial spare respiratory capacity (SRC)
- IL-15 regulates SRC by promoting mitochondrial biogenesis and CPT1a expression
- SRC in $CD8^+$ T_M cells is dependent on mitochondrial fatty acid oxidation (FAO)
- Mitochondrial FAO enhances T cell survival and promotes $CD8^+$ T_M cell development

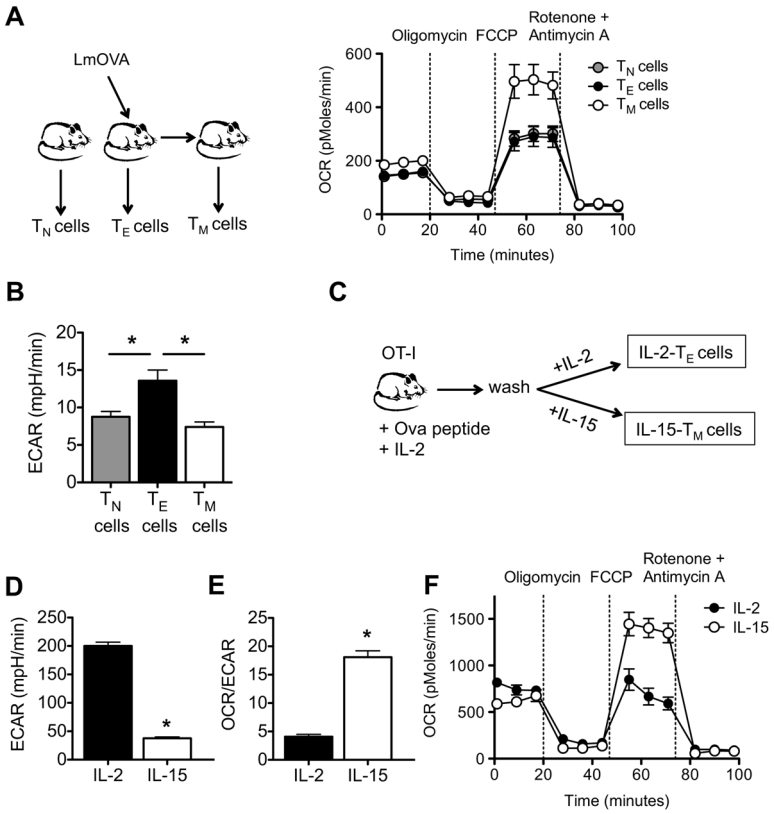

Figure 1. CD8$^+$ T_M cells have substantial mitochondrial spare respiratory capacity

Spleens and lymph nodes were harvested from naive and LmOVA infected mice, and T_N, T_E, and T_M cells were isolated. (**A**) O_2 consumption rates (OCR) were measured in real time under basal conditions and in response to indicated mitochondrial inhibitors; $P < 0.0001$ after FCCP injection. Data are representative of 4 independent experiments. (**B**) Extracellular acidification rates (ECAR) were measured under basal conditions; *$P < 0.01$ for T_E versus T_N cells, and < 0.01 for T_E versus T_M cells. Data are representative of 2 independent experiments. (**C-F**) OT-I cells were activated with OVA peptide for 3 days, and subsequently cultured in either IL-2 or IL-15 to generate IL-2 T_E and IL-15 T_M cells, respectively. Basal extracellular acidification rate (ECAR) (**D**), basal OCR/ECAR ratio (**E**), and OCR under basal conditions and in response to indicated mitochondrial inhibitors (**F**) in IL-2 T_E and IL-15 T_M cells are shown; *$P < 0.0001$ (D), < 0.0001 (E), <0.0001 (F after FCCP). Data are representative of at least 3 independent experiments. Data are shown as mean ± SEM. See also Figure S1.

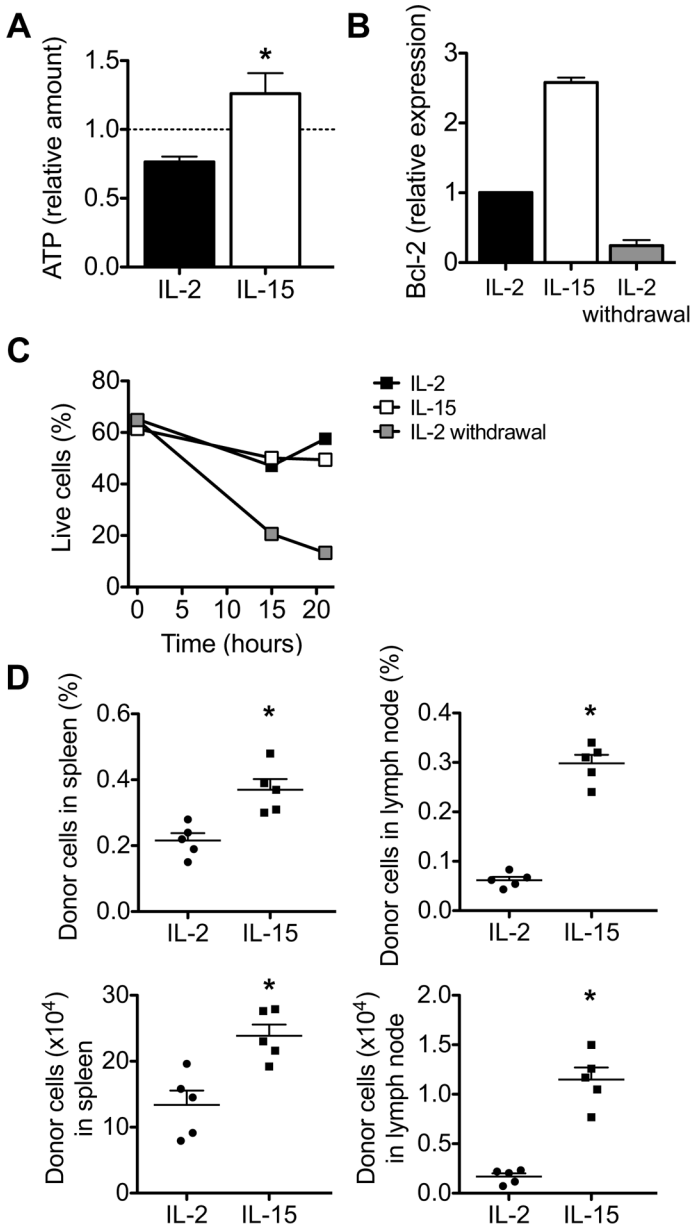

Figure 2. IL-15 signals promote CD8$^+$ T cell survival

OT-I cells were activated with OVA peptide for 3 days, and subsequently cultured in either IL-2 or IL-15. (**A**) IL-2 T_E and IL-15 T_M cells were re-stimulated with anti-CD3 and anti-CD28 for 5 hours and the amounts of re-stimulation induced ATP are shown relative to non-re-stimulated cells (dashed line); **P* = 0.03. Data are shown as mean ± SEM and are representative of 2 independent experiments. (**B-C**) IL-2 cultured cells were withdrawn from IL-2 for 6–8 hours, and (**B**) relative Bcl-2 mRNA expression and (**C**) percentage live cells (based on 7-AAD analysis) are shown. Data are shown as the mean ± SEM (figure generated from 2 independent experiments) (B) or as a representative experiment of 3 independent experiments (C). (**D**) IL-2 T_E and IL-15 T_M cells were adoptively transferred into congenic recipients (*n* = 5 per group), and organs were harvested 2 days later, dot plots show percentages, *top panels*, or total numbers, *bottom pane*ls, of donor cells. Data are shown as

mean ± SEM. Data are representative of 2 independent experiments. *P = 0.004 (top left), < 0.0001 (top right), 0.005 (bottom left), and < 0.0001 (bottom right). See also Figure S2.

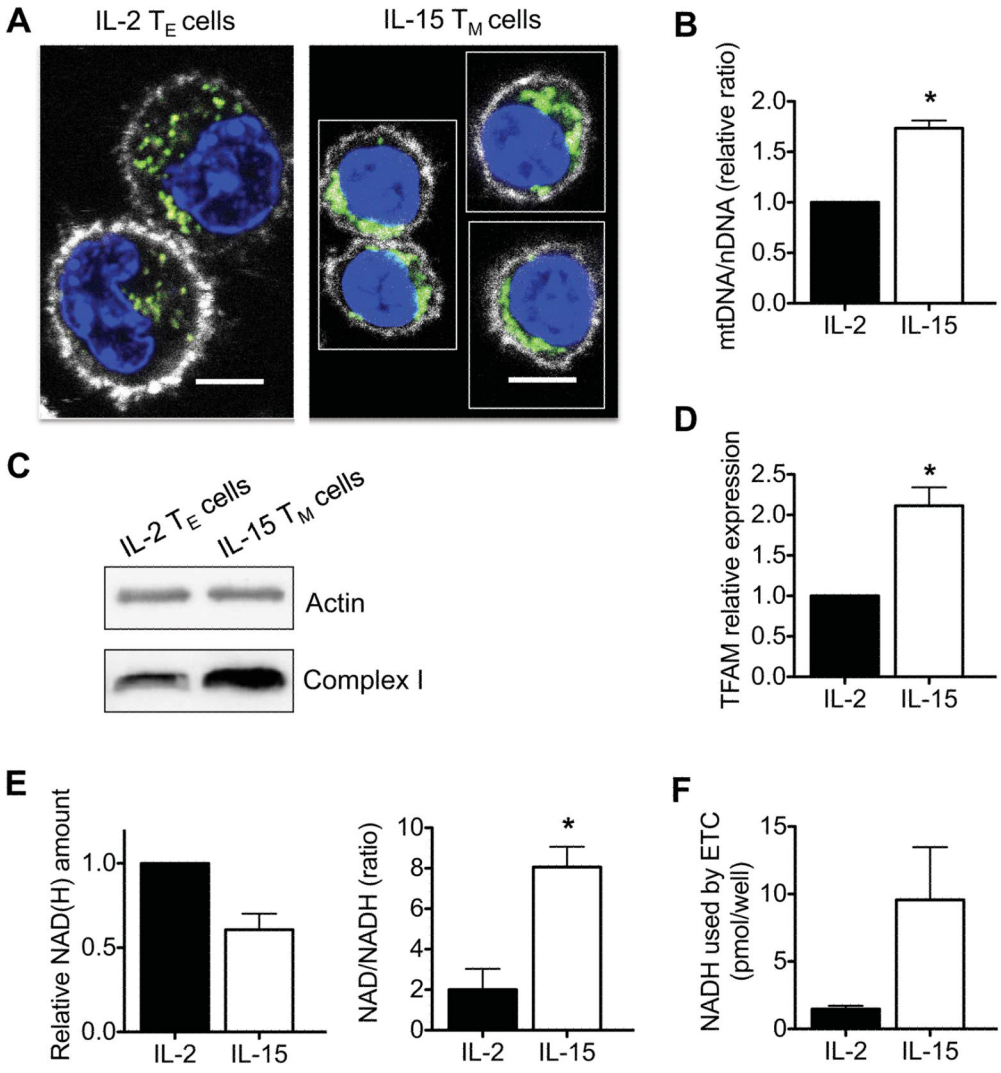

Figure 3. IL-15 induces mitochondrial biogenesis in CD8 $^{+}$T cells

IL-2 T_E and IL-15 T_M cells were analyzed (A-F). (**A**) Confocal images show cells stained with Mitotracker (green), Hoechst (blue), and anti-CD8 (white), scale bars are 5 microns. (**B**) mtDNA/nDNA ratio (figure generated from 2 independent experiments) *P = 0.01, (**C**) Western analysis for complex I expression, and (**D**) relative mitochondrial transcription factor A (TFAM) mRNA expression (figure generated from 5 independent experiments) in IL-2 T_E and IL-15 T_M cells; *P = 0.008. (**E**) Relative total amount of NAD(H), NAD/NADH ratio, and (**F**) NADH consumed by the ETC (measured as NADH built up after ETC blockade) in IL-2 T_E and IL-15 T_M cells (figures generated from 3 independent experiments); *P = 0.03. Data are shown as mean ± SEM. Data in A and C are representative of at least 3 independent experiments. See also Figure S3.

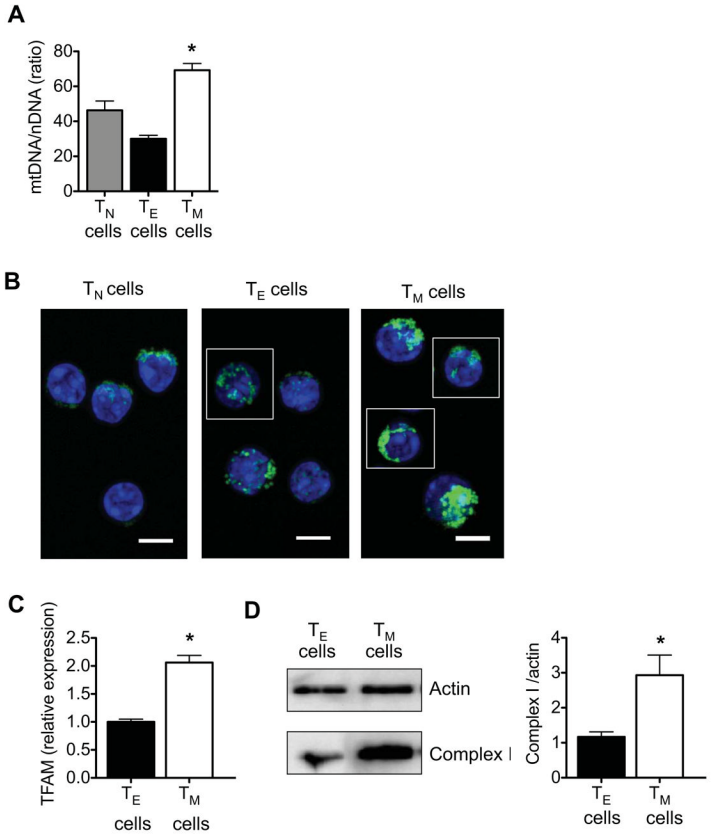

Figure 4. CD8$^+$ T_M cells have greater mitochondrial mass than CD8$^+$ T_E cells

Spleens and lymph nodes were harvested from naive and LmOVA infected mice, and T_N, T_E, and T_M cells were isolated. (**A**) mtDNA/nDNA ratio (data are shown as mean ± SEM, figure generated from 2 independent experiments) *P < 0.01 for T_E vs T_M cells, and < 0.05 for T_N vs T_M cells. (**B**) Confocal images show T_N, T_E and T_M cells stained with Mitotracker (green) and Hoechst (blue), scale bars are 5 microns. (**C**) Relative mitochondrial transcription factor A (TFAM) mRNA expression (data are shown as mean ± SEM, figure generated from 2 independent experiments) *P = 0.01, and (**D**) Western analysis for complex I expression (bars depict quantification of densitometry from 3 blots) *P = 0.008. Data are representative of 2 independent experiments.

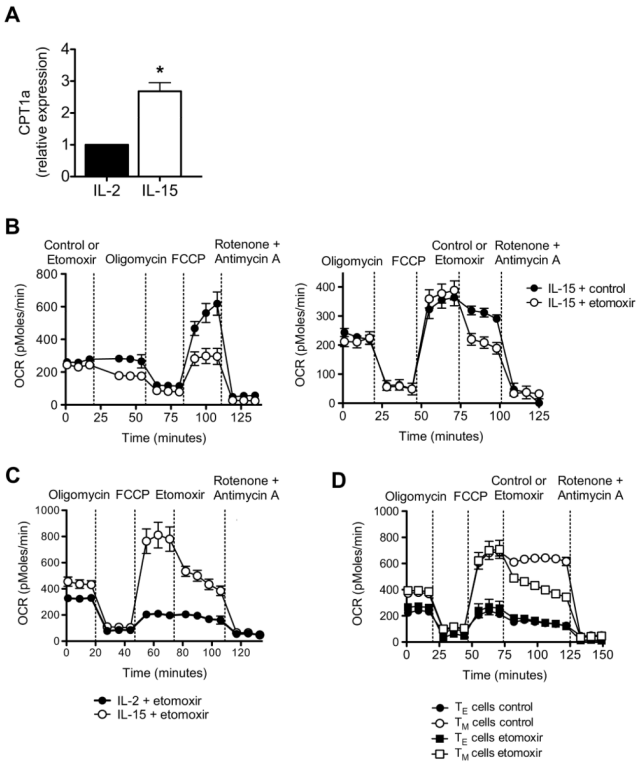

Figure 5. Spare respiratory capacity in CD8$^+$ T cells is dependent on mitochondrial FAO

(**A**) Relative CPT1a mRNA expression in IL-2 T_E and IL-15 T_M cells (figure generated from data from 5 independent experiments); **P* = 0.003. Oxygen consumption rates (OCR) in IL-15 T_M cells (**B**), in IL-2 T_E and IL-15 T_M cells (**C**), and *bona fide* T_E and T_M cells isolated from LmOVA infected B6 mice (**D**), under basal conditions and in response to indicated drugs; $P < 0.0001$ (after FCCP in B left panel), < 0.01 (after etomoxir in B right panel), and < 0.0001 (for T_M cells after etomoxir versus control, D). See also Figure S4.

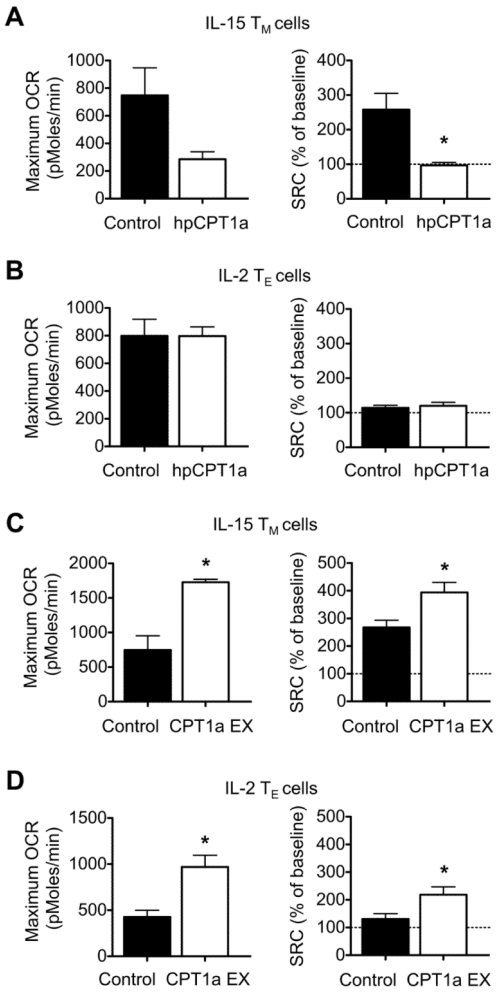

Figure 6. Spare respiratory capacity in CD8$^+$ T cells is dependent on CPT1a expression

Maximum OCR (as indicated by OCR after injection of oligomycin and subsequent FCCP) and spare respiratory capacity (indicated by maximum OCR calculated as percentage of baseline OCR) in IL-15 T_M cells(**A, C**) and IL-2 T_E cells (**B, D**) cells transduced with either control (virus expressing shRNA against luciferase) or virus expressing shRNA against CPT1a (hpCPT1a) (**A, B**), and either control (empty vector) or CPT1a expressing (EX) retrovirus (**C, D**); **P* = 0.03 (A), 0.003 (max OCR) and 0.02 (SRC) (C), 0.006 (max OCR) and 0.03 (SRC) (D). Data are representative of at least 2 independent experiments, and shown as mean ± SEM. See also Figure S5.

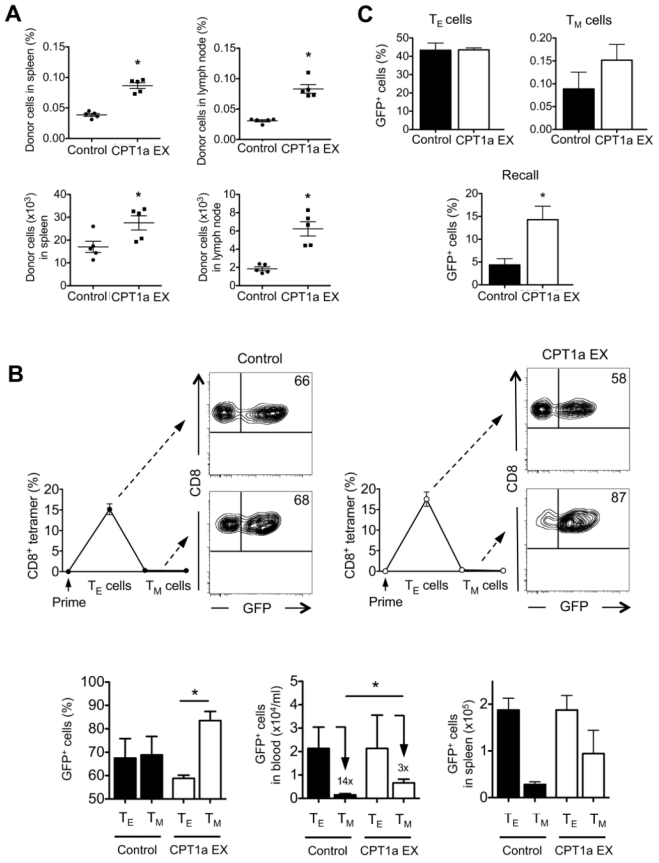

Figure 7. Mitochondrial FAO enhances T cell survival and promotes CD8$^+$ T_M cell development

OVA peptide activated OT-I cells transduced with control (empty vector) or CPT1a expressing (EX) retrovirus were intravenously injected into congenic recipients (n = 5 per group), and (**A**) organs were harvested 2 days later, dot plots show percentages (top panels), or total numbers (bottom panels) of donor cells (mean ± SEM); *P < 0.0001 (top left), < 0.0001 (top right), 0.03 (bottom left), and 0.0006 (bottom right), or (**B**) mice were infected with LmOVA, and peripheral blood CD8$^+$ T cells were analyzed by K^{b}OVA tetramer (line graphs) and GFP for retroviral expression (contour plots) at the peak of the response (T_E cells, day 7) and after contraction (T_M cells, day 14). Contour plots and bar graphs show the frequency of transduced (GFP$^+$) cells within the CD8$^+$ and K^{b}OVA tetramer positive gate in blood (left bar graph; *P = 0.0003), absolute numbers of transduced (GFP$^+$) cells/ml blood (middle bar graph, data are normalized to control T_E cells; P = 0.02, numbers above bars indicate fold contraction), and absolute numbers of transduced (GFP$^+$) cell in spleen (right bar graph, data are normalized to control T_E cells). Data are shown as mean ± SEM and are representative of at least 2 independent experiments with at least 5 mice per group. (**C**) OT-I cells transduced with control (empty vector) or CPT1a expressing (EX) retrovirus were intravenously injected into IL-15 deficient recipients (n = 5 per group) and mice were infected with LmOVA. Bar graphs show the frequency of transduced (GFP$^+$) cells within the K^{b}OVA tetramer gate at the peak of the response (T_E cells, day 7), after contraction (T_M cells, day 14) and after challenge (recall, day 5 post challenge); *P = 0.01. Data are shown as mean ± SEM and are representative of 2 independent experiments. See also Figure S6.